Int. J. Dev. Biol. 59: 313-325 (2015)
doi: 10.1387/ijdb.150206am

THE INTERNATIONAL JOURNAL OF DEVELOPMENTAL BIOLOGY
www.intjdevbiol.com

Two-Pore Channel 2 activity is required for slow muscle cell-generated Ca^{2+} signaling during myogenesis in intact zebrafish

JEFFREY J. KELU[1], HAYLEY L.H. CHAN[2], SARAH E. WEBB[1], ARTHUR H.H. CHENG[1,#], MARGARIDA RUAS[2], JOHN PARRINGTON[2], ANTONY GALIONE[2] and ANDREW L. MILLER*[,1,3]

[1]*Division of Life Science & State Key Laboratory of Molecular Neuroscience, HKUST, Clear Water Bay, Hong Kong, PRC,* [2]*Department of Pharmacology, University of Oxford, Mansfield Road, Oxford, UK and* [3]*MBL, Woods Hole, MA, USA*

ABSTRACT We have recently characterized essential inositol 1,4,5-trisphosphate receptor (IP_3R) and ryanodine receptor (RyR)-mediated Ca^{2+} signals generated during the differentiation of slow muscle cells (SMCs) in intact zebrafish embryos. Here, we show that the lysosomal two-pore channel 2 (TPC2) also plays a crucial role in generating, and perhaps triggering, these essential Ca^{2+} signals, and thus contributes to the regulation of skeletal muscle myogenesis. We used a transgenic line of zebrafish that expresses the bioluminescent Ca^{2+} reporter, aequorin, specifically in skeletal muscle, in conjunction with morpholino (MO)-based and pharmacological inhibition of TPC2, in both intact embryos and isolated SMCs. MO-based knock-down of TPC2 resulted in a dramatic attenuation of the Ca^{2+} signals, whereas the introduction of *TPCN2*-MO and *TPCN2* mRNA together partially rescued the Ca^{2+} signaling signature. Embryos treated with *trans*-ned-19 or bafilomycin A1, a specific NAADP receptor inhibitor and vacuolar-type H^+ ATPase inhibitor, respectively, also displayed a similar disruption of SMC Ca^{2+} signaling. TPC2 and lysosomes were shown via immunohistochemistry and confocal laser scanning microscopy to be localized in perinuclear and striated cytoplasmic domains of SMCs, coincident with patterns of IP_3R and RyR expression. These data together imply that TPC2-mediated Ca^{2+} release from lysosomes acts upstream from RyR- and IP_3R-mediated Ca^{2+} release, suggesting that the former might act as a sensitive trigger to initiate the SR-mediated Ca^{2+}-induced-Ca^{2+}-release essential for SMC myogenesis and function.

KEY WORDS: *two-pore channel 2, Ca^{2+} signaling, slow muscle cell myogenesis, zebrafish, in vivo imaging*

Introduction

Ca^{2+} is a highly versatile intracellular messenger that regulates various cellular and developmental functions (Berridge, 2012). While its requirement during mature muscle contraction has long been known (Ringer, 1882), evidence is now accumulating to suggest that Ca^{2+} signaling also plays a critical role in many aspects of myogenesis. Most of these latter reports, however, result from experiments carried out on isolated muscle cells in culture (Jaimovich *et al.*, 2000; Aley *et al.*, 2010), with only a few experiments conducted in muscle cells differentiating *in situ* and thus subjected to multiple 3D signaling cues from the surrounding tissues and extracellular matrix. A limited number of *in vivo* studies in zebrafish do, however, report that a series of highly reproducible Ca^{2+} signals generated in the developing skeletal myotome have a distinct pattern with respect to location, frequency, amplitude, and duration, and that they are essential for myofibrilogenesis (Brennan *et al.*, 2005; Cheung *et al.*, 2011). Using fluorescent Ca^{2+} reporters,

Abbreviations used in this paper: AChR, acetylcholine receptor; cADPR, cyclic adenosine diphosphate ribose; CICR, Ca^{2+}-induced Ca^{2+} release; EC, excitation-contraction; ET, excitation-transcription; hpf, hours post-fertilization; IP_3R, inositol 1,4,5-trisphosphate receptor; LAMP1, lysosomal-associated membrane protein 1; MO, morpholino antisense oligonucleotide; NAADP, nicotinic acid adenine dinucleotide diphosphate; RyR, ryanodine receptor; SMC, slow muscle cell; SP, signaling period; SR, sarcoplasmic reticulum; TPC2, two-pore channel 2.

***Address correspondence to:** Andrew L. Miller. Division of Life Science, HKUST, Clear Water Bay, Kowloon, Hong Kong. Tel: +852 2358 8631; Fax: +852 2358 1559. E-mail: almiller@ust.hk - web: http://ihome.ust.hk/~aequorin

[#]Present address: Department of Biology, University of Toronto Mississauga, Mississauga, Ontario, Canada. L5L 1C6.

Accepted: 20 July 2015.

ISSN: Online 1696-3547, Print 0214-6282

Brennan *et al.,* (2005) reported that between ~17 to 22 hours post-fertilization (hpf), acetylcholine (ACh) released from primary motor neurons triggers Ca^{2+}-induced Ca^{2+} release (CICR) via ryanodine receptors (RyR), which then initiates spontaneous contractions of slow muscle cells (SMCs) in the developing myotome. In addition, myofibril organization, but not the number of SMCs, or their elongation and migration, was affected when the ACh receptor (AChR) or RyR were blocked using α-bungarotoxin or inhibitory concentrations of ryanodine, respectively. They proposed, therefore, that in intact zebrafish, Ca^{2+} signals generated in differentiating SMCs play a key role in regulating myofibrilogenesis (Brennan *et al*., 2005). Cheung *et al.,* (2011) then extended this study, (using aequorin-based luminescence Ca^{2+} imaging), and reported that not one, but two distinct periods of Ca^{2+} signaling are found between ~17.5 hpf and 24 hpf during SMC development. Furthermore, using complementary high-resolution fluorescence-based Ca^{2+} imaging, they also showed that distinct Ca^{2+} signals are generated in both the nucleus and cytoplasm of SMCs between ~17.5 hpf to 19.5 hpf (Signaling Period, SP, 1), whereas cytoplasmic Ca^{2+} signals predominate after ~24 hpf (SP2; Cheung *et al*., 2011). Using a pharmacological approach, the early SP1 nuclear component was blocked by an appropriate concentration of 2-aminoethoxydiphenyl borate (2-APB) and was thus suggested to be mediated mainly via inositol 1,4,5-trisphosphate receptors (IP_3Rs). Conversely, the cytoplasmic component of both SP1 and SP2 that was associated with SMC contraction was blocked by inhibitory concentrations of ryanodine, suggesting that it is mediated mainly by RyRs. As well as blocking the distinct patterns and frequencies of Ca^{2+} signals generated in SMCs, inhibition of IP_3R and RyR activity also disrupted SMC myofibrilogenesis (Brennan *et al*., 2005; Cheung *et al*., 2011), suggesting a critical role for the distinct Ca^{2+} signaling signatures generated during the development and differentiation of SMCs in intact zebrafish.

Currently, three major endogenous Ca^{2+} mobilizing messengers have been described: inositol-1,4,5-trisphosphate (IP_3), cyclic adenosine diphosphate ribose (cADPR), and nicotinic acid adenine dinucleotide diphosphate (NAADP; Bootman *et al*., 2002). While it has long been known that NAADP targets acidic Ca^{2+} stores, which are distinct from the SR/ER (Churchill *et al*., 2002; Galione and Ruas, 2005), the identity of the NAADP target channel has only recently been established. Accumulating evidence suggests that members of the two-pore channel (TPC) family, which are found on the membrane of endo-lysosomal vesicles, are targets for NAADP-induced Ca^{2+} release (Menteyne *et al*., 2006; Calcraft *et al*., 2009). In most vertebrates, including zebrafish, there are three distinct TPCs; TPC1 and TPC3 are localized in endosomes and other compartments of the endo-lysosomal system, whereas TPC2 is predominantly found in late endosomes and lysosomes (Ruas *et al*., 2014). Although two recent reports have challenged the proposal that TPC1 and TPC2 are NAADP-regulated channels (Wang *et al*., 2012; Cang *et al*., 2013), more recent work has confirmed that NAADP can indeed activate TPC2 at least to mediate Ca^{2+} release (Jha *et al*., 2014). These and other recent reports indicate that the regulation of TPC activity is likely to be more complex than was originally proposed (Morgan and Galione, 2014; Jha *et al*., 2014).

Following the discovery of TPCs, several reports have indicated a role for TPC-mediated Ca^{2+} signaling in the differentiation (Parrington and Tunn, 2014) and function (Tugba Durlu-Kandilci *et al*., 2010) of different types of vertebrate muscle fibers. However, once again these experiments were conducted mainly in isolated cultured cells. Here, we present the first *in vivo* evidence that TPC2 plays a key role in myogenesis in an intact vertebrate. Utilizing an α-actin-aequorin transgenic zebrafish line, where apoaequorin is expressed specifically in the trunk skeletal musculature (Cheung *et al*., 2011), we used MO-based knockdown and pharmacological inhibition of TPC2 to determine its role in generating the SMC Ca^{2+} signals and in myogenesis. Rescue of the Ca^{2+} signaling signature of the morphants was also performed by co-injecting *TPCN2*-mRNA to validate the specificity of action of the *TPCN2*-MO. Immunohistochemistry was used to determine the localization of TPC2 in intact embryos at different developmental stages. In order to verify the fidelity of these results, the localization of TPC2 and lysosomes was then visualized in primary muscle cells cultured from embryos at ~17-somite stage. The spatial relationship between TPC2, RyR, IP_3R, sarcomeric organization, and the nucleus in cultured muscle cells was also determined. We suggest that the co-localization of these various Ca^{2+} release channels in the nuclear and cytoplasmic domains in cultured cells is recapitulated in the intact myotome, where they may represent distinct trigger zones for generating the essential myogenic Ca^{2+} signals that are required for excitation-transcription (ET) coupling as well as excitation-contraction (EC) coupling.

Results

Effect of MO-based knockdown and mRNA rescue of TPC2 on the SMC-generated Ca^{2+} signals

Endogenous Ca^{2+} signals generated in SMCs during normal embryogenesis between ~17 hpf and 30 hpf are shown in Fig. 1Ai and Fig. 1F, a representative example and the mean ± SEM of five experiments, respectively. The graphs confirm the occurrence of the SP1, a quiescent period (QP) and SP2 (Cheung *et al*., 2011), and demonstrate that SP2 extends beyond ~24.5 hpf as previously reported, to at least 30 hpf. When embryos were injected with a standard control-MO, a similar pattern of SP1, QP and SP2 Ca^{2+} signals was observed (Fig 1Bi, 1G). When embryos were injected with *p53*-MO, distinct SP1, QP and SP2 were again observed (Fig. 1Ci, 1H). When embryos were injected with a mixture of *TPCN2*-MO and *p53*-MO, however, the SP1 and SP2 Ca^{2+} signals were completely inhibited (Fig. 1Di, 1I). Addition of Triton X-100 at the end of the experiment indicates that the lack of luminescence signal observed (Fig. 1Di) was due to the Ca^{2+} signals being inhibited rather than from a lack of unreacted aequorin in embryos (Fig. 1Dii). When embryos were injected first with *TPCN2*-MO and *p53*-MO, and then with *TPCN2*-mRNA in order to attempt to rescue the effect of TPC2 inhibition, a partial rescue of both the SP1 and SP2 Ca^{2+} signals occurred (Fig. 1Ei, 1J). Again, Triton X-100 addition at the end of the rescue experiment (Fig. 1Eii) indicated that sufficient active aequorin was present during the imaging period and thus the partial rescue of the Ca^{2+} signals generated was a real effect and not due to a lack of unreacted aequorin.

Effect of bafilomycin A1 and trans-ned-19 on the SMC-generated Ca^{2+} signals

In addition to the inhibition of TPC2 via an MO-based methodology, we also used a pharmacological approach, with bafilomycin A1 (a vacuolar-type H^+ ATPase inhibitor) and *trans*-ned-19 (a specific

NAADP receptor inhibitor), to determine the contribution made by NAADP and acidic stores to Ca^{2+} signaling during SMC formation. Untreated embryos were observed until the first SP1 Ca^{2+} signals were detected. At this point, embryos were removed from the photomultiplier tube (PMT); the tip of the tail was surgically removed; and the normal bathing medium changed to one containing either bafilomycin A1 or *trans*-ned-19. This procedure normally took ~15 min after which data acquisition was resumed. The Ca^{2+} signals generated by an embryo treated with 1.25% DMSO between ~18 hpf and 30 hpf are shown in Fig. 2Ai, 2D. When embryos were treated with 1 μM bafilomycin A1 from shortly after the SP1 signals were observed until 30 hpf, the remaining SP1 was inhibited, such that the normal high-frequency Ca^{2+} signals ended by ~18.5 hpf (Fig. 2Bi, 2E). A few small Ca^{2+} signals were generated between ~19 hpf and ~21 hpf but the SP2 Ca^{2+} signals were completely inhibited (Fig. 2Bi, 2E). When embryos were treated with *trans*-ned-19 from shortly after the SP1 signals were observed until 30 hpf, the remaining SP1 as well as SP2 Ca^{2+} signals were inhibited (Fig. 2Ci, 2F). The addition of Triton X-100 at the end of these experiments indicated once again that the absence of luminescence was due to the Ca^{2+} signals being inhibited rather than a lack of active aequorin (Fig. 2Bii, 2Cii).

Localization of TPC2 in the SMCs of intact control, MO-knockdown, and rescued embryos

Figure 3 A-E shows the development of TPC2 labeling between

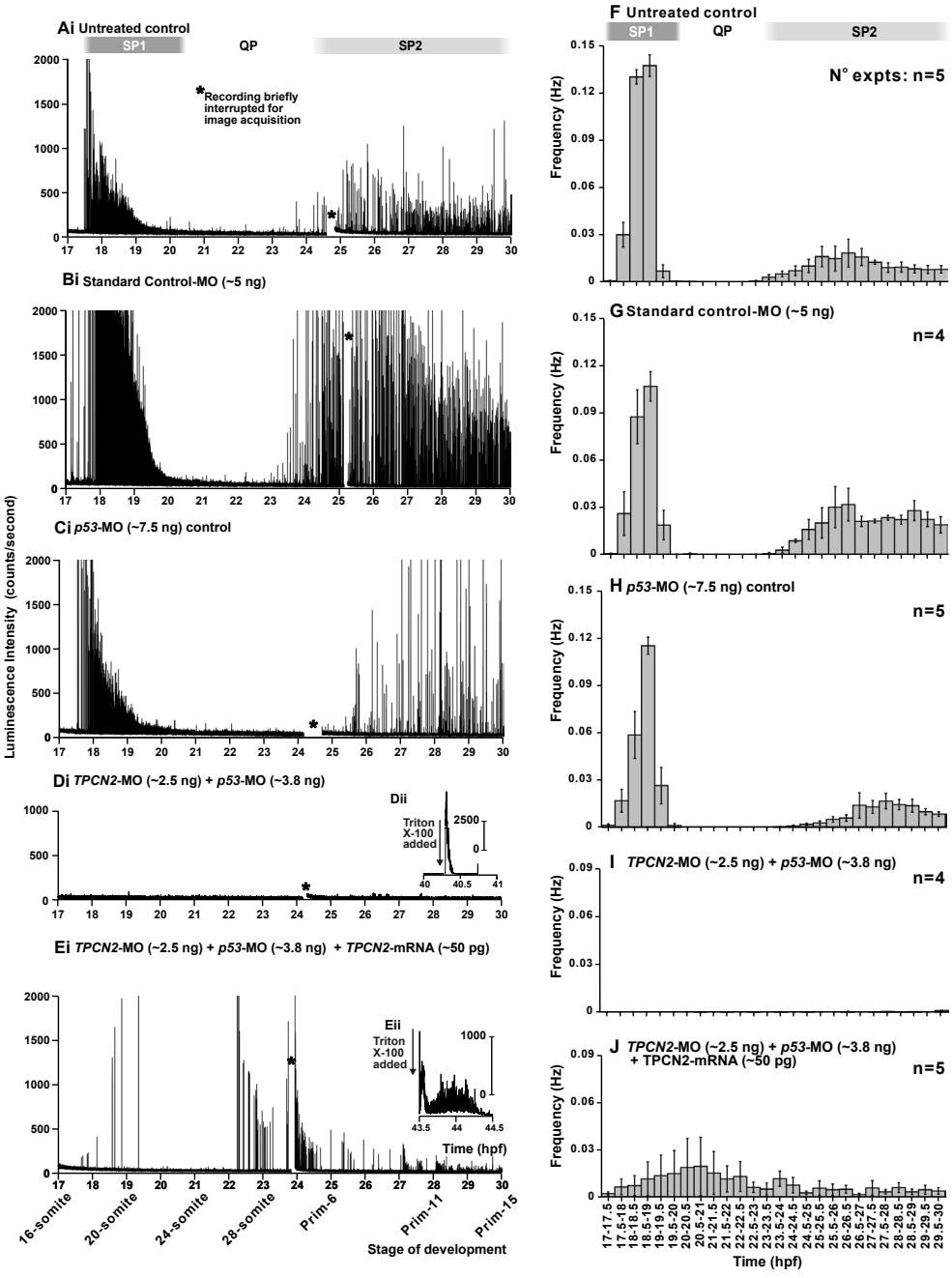

Fig. 1. Effect of MO-based knockdown of TPC2 on the SMC-generated Ca^{2+} signals from 17 hpf to 30 hpf. *Representative temporal profiles of the luminescence generated by α-actin-aeq transgenic embryos that were* **(Ai)** *untreated, or injected at the 1-4-cell stage with:* **(Bi)** *standard control-MO;* **(Ci)** p53-*MO;* **(Di)** TPCN2-*MO plus* p53-*MO; or* **(Ei)** TPCN2-*MO plus* p53-*MO, and* TPCN2-*mRNA at the amounts shown.* **(Dii, Eii)** *Temporal profiles of the luminescence when Triton X-100 was used at the end of each imaging experiment.* **(F-J)** *Histograms showing the mean ± SEM frequency of the Ca^{2+} signals generated every 30 min in the trunk musculature from 17 hpf to 30 hpf in embryos treated as described in panels A-E, respectively. Calcium signaling periods 1 and 2 (SP1 and SP2), and the signaling quiet period (QP; Cheung* et al.*, 2011) are shown.*

16 hpf and 24 hpf in normal untreated embryos. In addition to labeling with the TPC2 antibody, embryos were co-labeled with the F59 myosin heavy chain antibody, which can be used at these early stages to specifically identify the SMCs (Devoto *et al.*, 1996). At 16 hpf, the low level of myosin heavy chain labeling (Fig. 3Ai) was accompanied by an even lower level of expression of TPC2 (Fig. 3Aii). This was confirmed by performing a line-scan analysis on the TPC2 image (Fig. 3Aiii), which showed a low and unchanging level of fluorescence intensity along the 20 μm length of the line (Fig. 3Aiv). The line was placed in a position on the TPC2 image where the equivalent myosin heavy chain image showed distinct (albeit a low level of) labeling. At 18 hpf, when the level of myosin heavy chain expression was more obvious along the length of a few individual SMCs (Fig. 3Bi), the expression of TPC2 was still relatively homogeneous although the level of fluorescence intensity appeared to be higher than at 16 hpf (compare Fig. 3Bii with 3Aii). These features were also shown in the line-scan graph (Fig. 3Biii, 3Biv). At 20 hpf, when prominent myosin heavy chain banding was observed (Fig. 3Ci), TPC2 expression in individual myofibers was more obvious (Fig. 3Cii), and hints of TPC2 banding were observed both in the image itself (see blue arrowheads in Fig. 3Cii) and in the line-scan (Fig. 3Ciii,3Civ). At 22 hpf and 24 hpf, when the banding pattern of myosin heavy chain was well formed along the length of each SMC (Fig. 3Di, 3Ei), clear TPC2 banding was also observed in the myofibers of these cells (see blue arrowheads in Fig. 3Dii, 3Eii). This pattern of TPC2 banding is also clearly shown in the line-scans (Fig. 3Diii,3Div, 3Eiii,3Eiv).

The effect of injecting the *TPCN2*-MO (in conjunction with the *p53*-MO) on TPC2 expression was also tested (Fig. 3 F-H). Embryos injected with standard control-MO (Fig. 3F) or *p53*-MO (Fig. 3G) and then fixed at 24 hpf showed a similar pattern of expression of both the myosin heavy chain and TPC2 as the untreated control embryos at 24 hpf (compare Fig. 3Fi and 3Gi with Fig. 3Ei; and Fig. 3Fii and 3Gii with Fig. 3Eii). The line-scan analyses performed also showed a similarity in TPC2 expression in the standard control-MO and *p53*-MO injected embryos when compared with the untreated controls (compare Fig. 3Fiv and 3Giv with Fig. 3Eiv). Embryos injected with both *TPCN2*-MO and *p53*-MO, however, exhibited a disruption in the expression of both myosin heavy chain (Fig. 3Hi) and TPC2 (Fig. 3Hii-3Hiv), but when embryos were injected first with *TPCN2*-MO and *p53*-MO, and then with *TPCN2*-mRNA, the normal pattern of expression of myosin heavy chain (Fig. 3Ii) and TPC2 (Fig. 3 Iii-Iiv) was rescued.

In normal untreated embryos, the organization of TPC2 at 24 hpf in relation to the myosin heavy chain is shown at higher magnification in Fig. 3J. When the myosin heavy chain (Fig. 3Ji) and TPC2 (Fig. 3Jii) images were merged (Fig. 3Jiii) and a line-scan analysis performed (Fig. 3Jiv), TPC2 appeared to be mainly intercalated between the myosin heavy chain-labeled A-bands in the I-band regions (blue arrowheads in Fig, 3Jiii, Jiv) and (in some cases but to a lesser extent) in the M-lines (see pink arrowheads in Fig. 3 Jiii-Jiv, and see Fig. 3K for a schematic of a sarcomere).

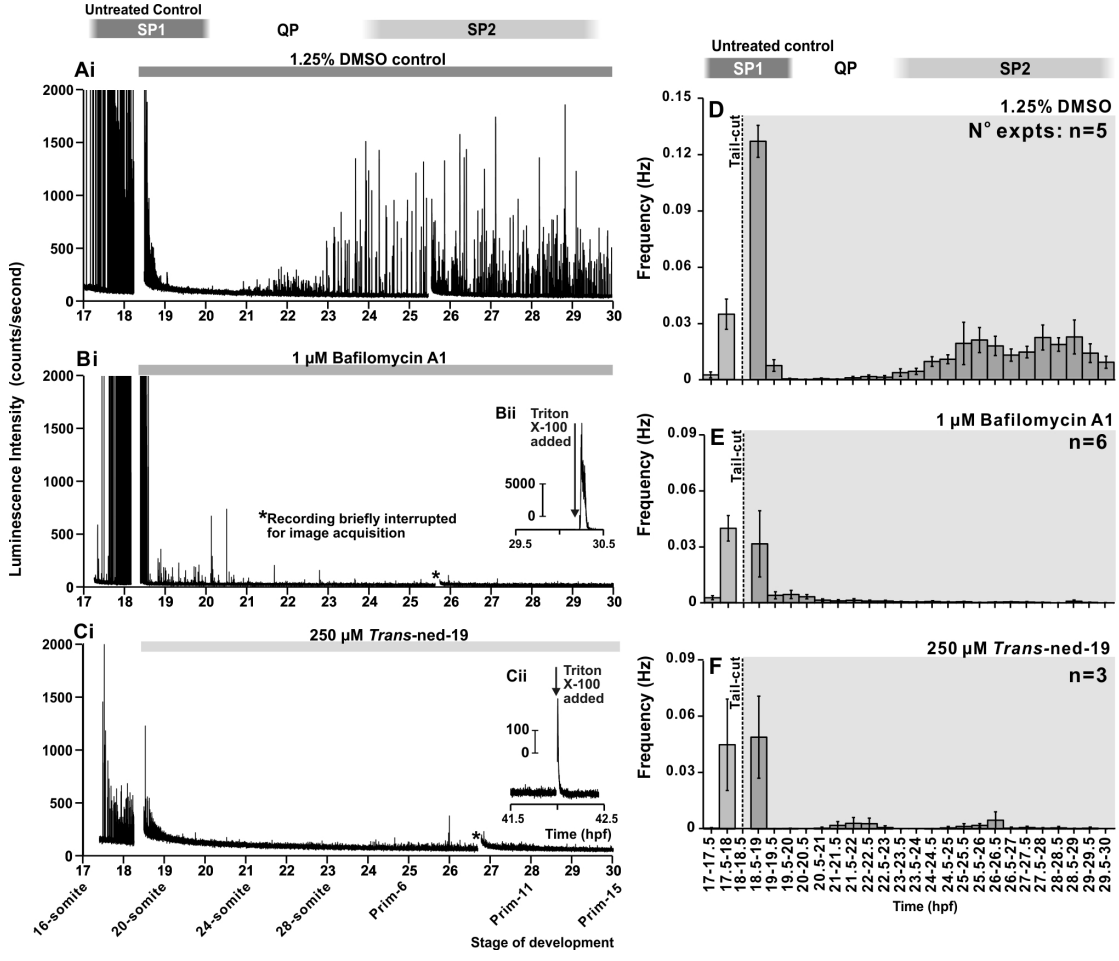

Fig. 2. Effect of bafilomycin A1 and *trans*-ned-19 on the SMC-generated Ca^{2+} signals from 17 hpf to 30 hpf. *Representative temporal profiles of the luminescence generated by α-actin-aeq transgenic embryos that were treated with* **(Ai)** *DMSO;* **(Bi)** *bafilomycin A1; or* **(Ci)** trans-*ned-19 at the concentrations shown, after the SP1 Ca^{2+} signals were first observed. To optimize the exposure of the muscles to the drugs, a small portion of the tail was removed from embryos just prior to treatment.* **(Bii, Cii)** *Temporal profiles of the luminescence generated following the addition of Triton X-100.* **(D-F)** *Histograms showing the mean ± SEM frequency of the Ca^{2+} signals generated every 30 min in the trunk musculature from 17 hpf to 30 hpf in embryos treated as described in panels A-C, respectively. The time of the tail-cut and duration of drug incubation are shown by the dotted line and grey shading, respectively. SP1, SP2 and the QP (Cheung* et al.*, 2011) for an untreated control embryo are also shown.*

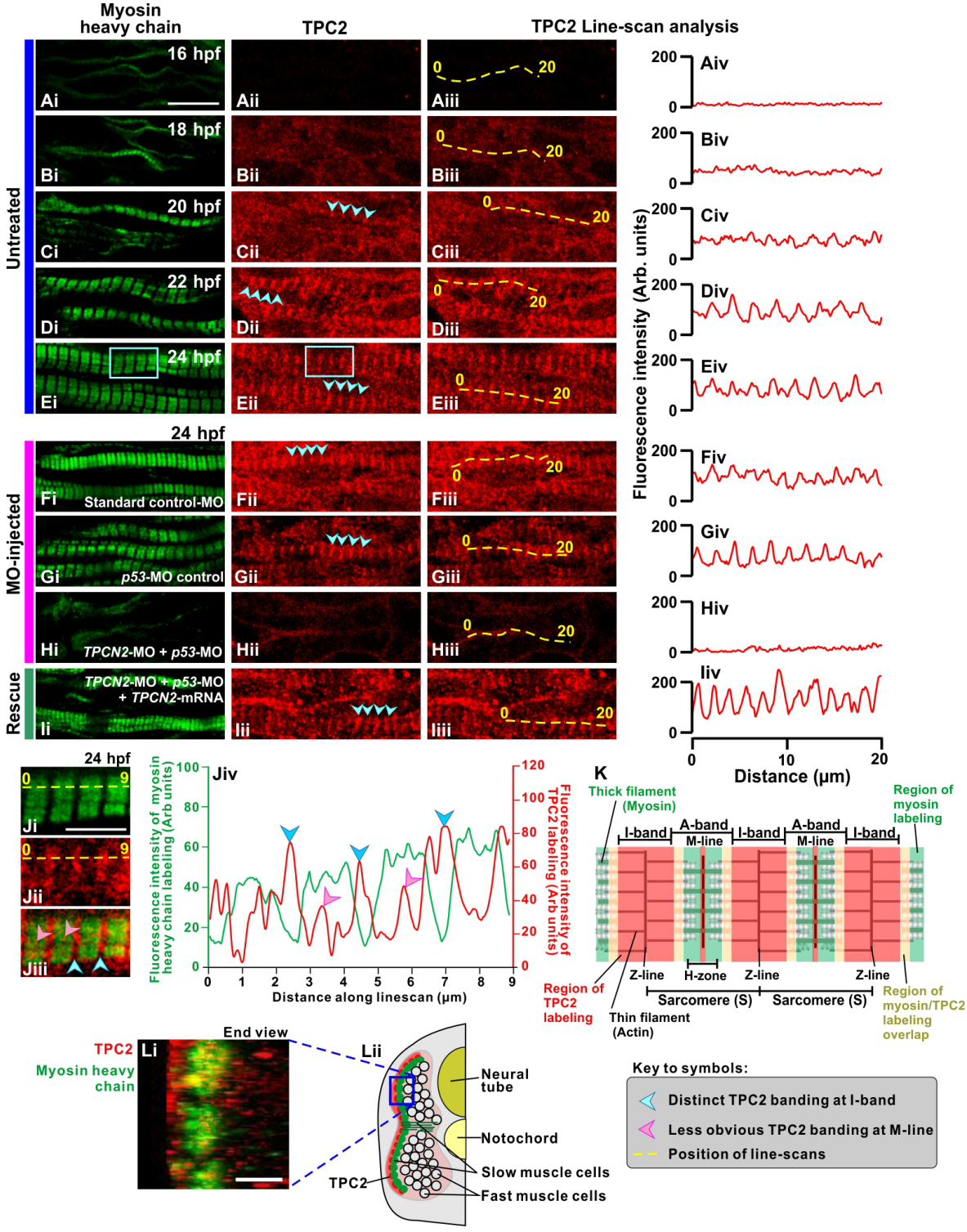

Fig. 3. Expression of TPC2 in the SMCs of intact embryos. *Embryos were fixed between 16 hpf and 24 hpf and then dual immunolabelled with a* **(Ai-Ii)** *myosin heavy chain and* **(Aii–Iii)** *TPC2 antibody.* **(F-I)** *Some embryos were injected with* **(F)** *standard control-MO,* **(G)** p53-*MO,* **(H)** TPCN2-*MO +* p53-*MO or* **(I)** TPCN2-*MO +* p53-*MO +* TPCN2-*mRNA between the 1-4-cell stage and then fixed at 24 hpf prior to immunolabeling.* **(Aiii–Iiii)** *Line-scan analyses were performed along individual myofibers and* **(Aiv-Iiv)** *graphs were plotted to show the development of TPC2 expression over time. The regions bounded by the blue rectangles in panels Ei and Eii are shown at higher magnification in panels Ji and Jii.* **(Jiii)** *The myosin heavy chain and TPC2 images when merged.* **(Jiv)** *Line-scan analysis showing the localization of TPC2 in relation to that of the myosin heavy chain in more detail.* **(K)** *Schematic representation of two sarcomeres.* **(Li)** *End view of several myofibers showing the localization of TPC2 in relation to the myosin heavy chain.* **(Lii)** *Schematic transverse section through an embryo at 24 hpf showing the location of TPC2 in relation to the SMCs and other cell types (modified from Fig. 1B in Du* et al., *1997). Scale bars, 10 μm (A-I); 5 μm (J, L).*

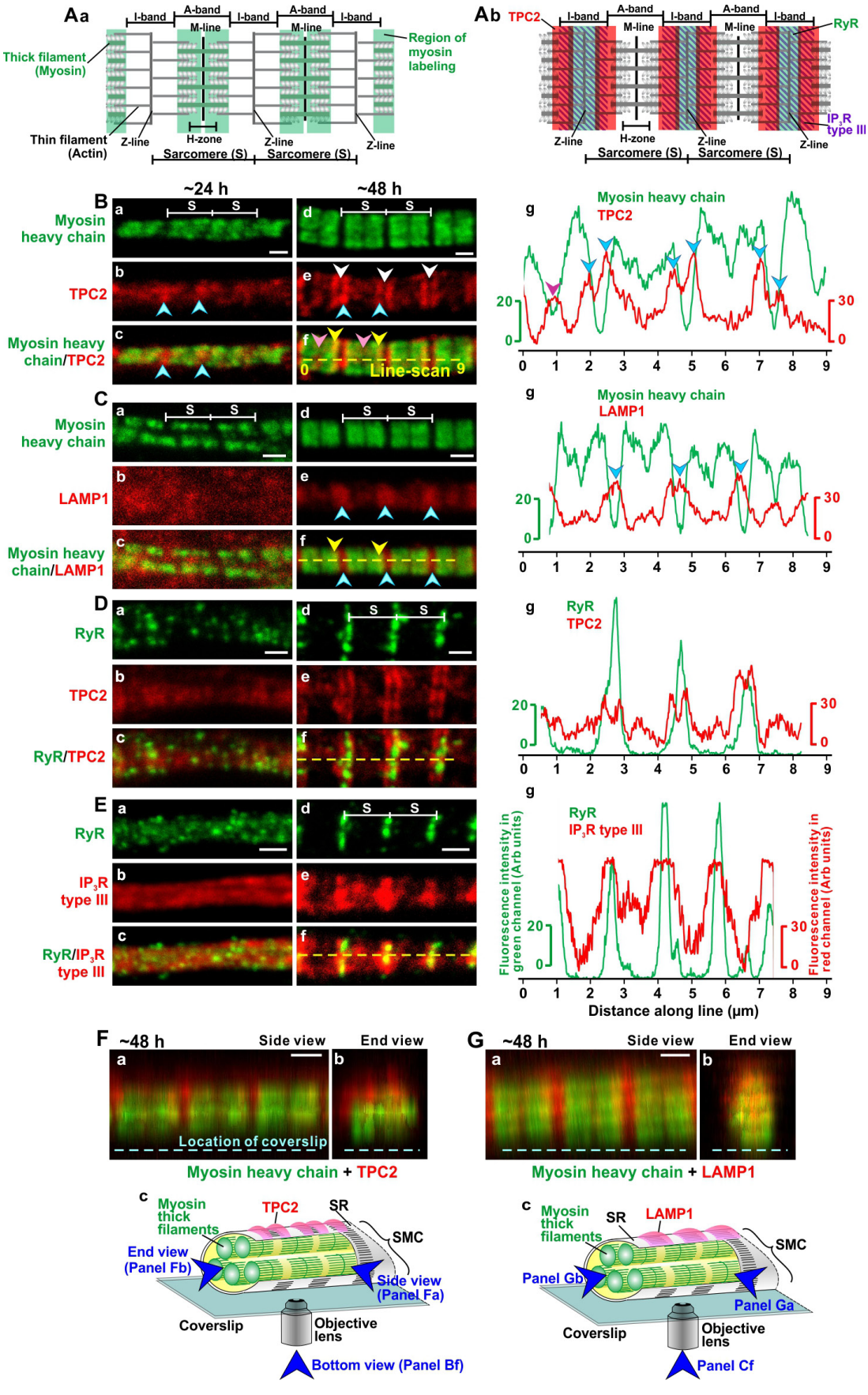

Fig. 4. Localization of TPC2 in the myofibers of primary cultures of SMCs. (A) *Schematic representations of two sarcomeres showing the localization of* **(Aa)** *myosin in green and* **(Ab)** *TPC2 (in red), RyR (in green) and IP_3R (diagonal shading).* **(B-E, panels a-f)** *Series of optical sections projected as single images to show the localization of TPC2 with regards to other proteins in the myofibrils or SR. Cells were dual-immunolabeled with:* **(B)** *myosin heavy chain and TPC2 antibodies;* **(C)** *myosin heavy chain and LAMP1 antibodies;* **(D)** *RyR and TPC2 antibodies; or* **(E)** *RyR and IP_3R type III antibodies. The pattern of localization is shown in cells cultured for either* **(B-E, panels a-c)** *~24 h or* **(B-E, panels d-f)** *~48 h, and for each series of antibodies used, the pattern of localization of each protein is shown both alone (panels a,d and b,e) and when superimposed on the image of the other protein labeled (panels c,f). Scale bars, 1 μm.* **(B-E, panel g)** *Line-scan analyses. See key to symbols in Fig. 3 for explanation of yellow dashed lines and the blue and pink arrowheads; white arrowheads indicate TPC2-exclusion zones around the sarcomeric z-line and yellow arrowheads indicate regions of TPC2 and myosin heavy chain overlap.* **(F,G)** *Side (panel a) and end (panel b) views of SMCs to show the localization of* **(F)** *TPC2 and* **(G)** *LAMP1 in relation to the myosin heavy chain.* **(F,G, panel c)** *Schematics to illustrate the different views observed.*

The relationship between TPC2 and myosin heavy chain was investigated in intact embryos by rotating projected images of TPC2/myosin heavy chain labeling by 90° vertically to provide an end view (Fig. 3Li). This showed that more TPC2 labeling was on the lateral side of the myofibrils within the SMCs (i.e., closest to the skin) than on the medial side (i.e., closest to the neural tube/notochord).

Localization of TPC2 in the myofibers of SMCs in primary culture

The localization of TPC2 in relation to the myosin heavy chain was also investigated in SMC primary cultures, which do not have the high background level of fluorescence observed in the whole-mount labeling experiments. TPC2 expression was less well organized in myofibers cultured for 24 h (Fig. 4Bb) than for 48 h (Fig. 4Be). However, when comparing the expression of TPC2 (Fig. 4Bb,4Be) with that of the myosin heavy chain (Fig. 4Ba,4Bd) in cells at both time points, it is clear that TPC2 was expressed in regions of the SMC that correlate with the sarcomeric I-band region (see blue arrowheads in Fig. 4Bc,4Bf,4Bg). Cells cultured for 48 h exhibited a more complex pattern of TPC2 localization in myofibers such that it appeared to be excluded from regions correlating to the sarcomeric z-line (see white arrowheads in Fig. 4Be), but there was some overlap with the A-band region (yellow arrowheads in Fig. 4 Bf). Furthermore, in some sarcomeres, TPC2 expression was also observed in the M-line region (pink arrowheads in Fig 4B f,g).

As TPC2 is reported to be localized to the lysosomes, the expression pattern of TPC2 in relation to lysosomal-associated membrane protein 1 (LAMP1) was also investigated (Fig. 4C). As both the LAMP1 and TPC2 antibodies were raised in rabbit, however, we could not directly immunolabel both proteins in the same cells. Thus, we again co-labeled cells with the F59 myosin heavy chain antibody (Fig. 4C a,d) and the LAMP1 antibody (Fig. 4C b,e). After 24 h in culture the expression of LAMP1 was relatively low and homogeneous (Fig. 4Cb) when compared with the expression of the myosin heavy chain where distinct sarcomeres were apparent (Fig. 4Ca). After 48 h in culture, however, LAMP1 expression was more organized, with a relatively diffuse pattern of labeling in regions of myofibers adjacent to the I-band (see blue arrowheads in Fig. 4C e-g) with a small amount of overlap with the A-band (see yellow arrowheads in Fig. 4Cf). Thus, TPC2 appears to be expressed in approximately the same region of the myofibers as LAMP1 (compare Fig. 4Bg and 4Cg).

The relationship between TPC2 and RyR was also investigated (Fig. 4D). After 24 h in culture, TPC2 expression was low and its distribution was homogeneous (Fig. 4Db) while RyR appeared as puncta along the myofibers (Fig. 4Da). After 48 h in culture, however, the sarcomeric banding pattern of both RyR and TPC2 was apparent; such that RyR were expressed adjacent to the z-line (Fig. 4D d,f,g) and TPC2 was expressed on either side of the RyR (Fig. 4D e-g). As the antibodies to TPC2 and IP_3R type III were both raised in rabbit, a direct comparison was not possible, thus cells were labeled with antibodies for RyR and IP_3R type III (Fig. 4E). After 24 h in culture IP_3R type III was expressed in a relatively uniform manner along the myofiber (Fig. 4Eb) while the RyR again showed a punctate labeling pattern (Fig. 4Ea). After 48 h in culture, IP_3R type III had a more diffuse pattern of localization than RyR, being expressed in a larger region of the I-band (compare Fig. 4Ee with Fig. 4Ed,Ef,Eg). A comparison of all these immunolabeling data suggests that TPC2 and LAMP1 appear to be expressed in a similar region of the myofibers as IP_3R type III.

The relationship between TPC2 or LAMP1 and the myosin heavy chain was investigated in further detail by rotating the projected images shown in Fig. 4Bf and 4Cf by 90° horizontally to provide a side view (Fig. 4Fa and 4Ga, respectively) and vertically to provide an end view (Fig. 4Fb and 4Ga, respectively). Both TPC2 and LAMP1 labeling were localized peripheral to the myosin heavy chain labeling but in an asymmetric manner such that both proteins were located on the side of the SMC furthest away from the coverslip. This is illustrated schematically in Fig. 4Fc and 4Gc.

Localization of TPC2 in the nucleus and peri-nuclear region of SMCs in primary culture

The localization of TPC2 and LAMP1 in relation to the nucleus was also investigated in primary SMCs cultured for 24 or 48 h (Fig. 5 A-D). For comparison, the localization of RyR and IP_3R type I, II and III was also determined (Fig. 5 E-H). All the images represent single optical sections acquired through a region of the cell where the nucleus was determined to be widest. In all the representative examples, images of the fluorescently labeled proteins are shown individually (panel a in Fig. 5 A-H and panel b in Fig. 5 E,F) and when merged into a single image with the DAPI-labeled nucleus (panel c in Fig. 5 A-D,G,H and panel d in Fig. 5 E,F). In addition, in each merged image, a yellow dashed line shows the position across the cell where the line-scan analysis was conducted. Figure 5A and 5B show the localization of TPC2 at 24 h and 48 h, respectively. At both time points, TPC2 was localized predominantly in the peri-nuclear region with a lower level of fluorescent labeling appearing in the nuclear region. The localization of LAMP1 at 24 h and 48 h is shown in Fig. 5 C,D, respectively. At 24 h, LAMP1 was localized entirely in the peri-nuclear region, with no expression being observed in the nucleus itself (Fig. 5C). On the other hand, at 48 h, LAMP1 was localized in both the nucleus and peri-nuclear region of the cell (Fig. 5D). Figure 5E and 5F show the localization of RyR and IP_3R type III at 24 h and 48 h, respectively. At both time points, both IP_3R type III and RyR were localized mainly in the peri-nuclear region, with relatively little labeling in the nucleus itself. In addition to IP_3R type III, the localization of IP_3R type I and IP_3R type II was also determined at 48 h (Fig. 5 G,H, respectively). Whereas IP_3R type I was localized within the nucleus alone (Fig. 5G), IP_3R type II was localized both in the nucleus and in the peri-nuclear region of the cell, with a more intense level of fluorescence occurring in the latter area (Fig. 5H).

Discussion

Here we report that after MO-mediated TPC2-knockdown, all SMC-generated Ca^{2+} signals in zebrafish embryos from ~17 hpf to 30 hpf were abolished (Fig. 1Di). We also showed that the Ca^{2+} signals were partially rescued by injecting a *TPCN2*-mRNA that is not recognized by the *TPCN2*-MO (Fig. 1Ei), which suggests that the action of the *TPCN2*-MO is specific. The morphants also showed severe disruption in the organization of the myosin heavy chain and TPC2 in the SMCs (Fig. 3H). This is somewhat similar to previous reports describing the effect of inhibitory concentrations of ryanodine on the organization of the trunk musculature (Brennan *et al.*, 2005; Cheung *et al.*, 2011). The results from our *TPCN2*-MO

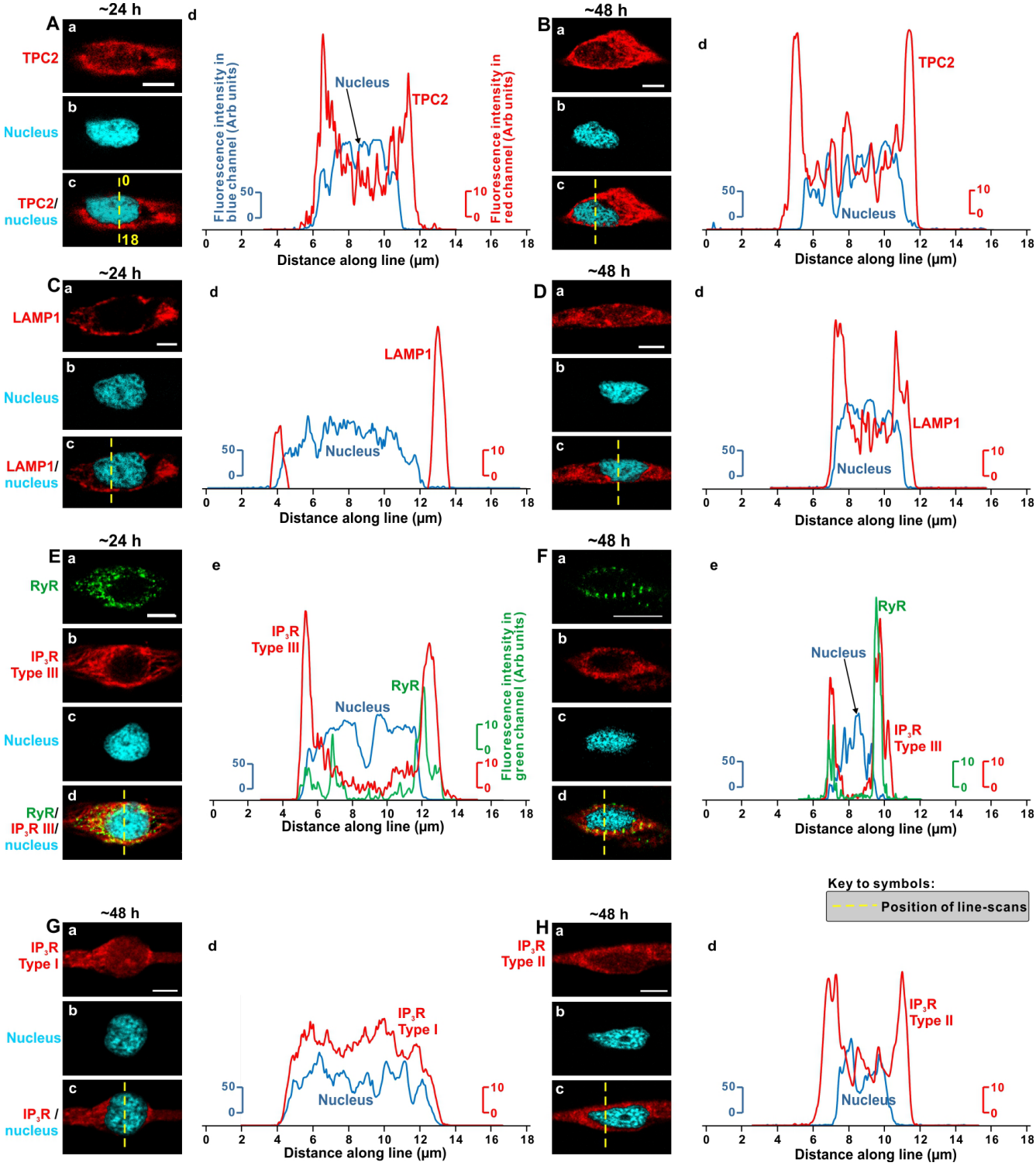

Fig. 5. Localization of TPC2 with respect to the nucleus and peri-nuclear region of SMCs. *Single optical sections (taken at the widest part of the nucleus) to show the localization of TPC2 and other proteins in the nuclear region of SMCs. Cells were dual-immunolabeled with:* **(A,B)** *myosin heavy chain and TPC2 antibodies;* **(C,D)** *myosin heavy chain and LAMP1 antibodies;* **(E,F)** *RyR and IP_3R type III antibodies,* **(G)** *myosin heavy chain and IP_3R type I antibodies or* **(H)** *myosin heavy chain and IP_3R type II antibodies, and then counterstained with DAPI to label the nucleus. In panels A-D, G and H the myosin heavy chain antibody was simply used to identify SMCs in the mixed cell culture (and is therefore not shown). In the case of TPC2, LAMP1, IP_3R type I and IP_3R type II, the localization pattern of these proteins was shown alone (A-D,G,H, panel a) and when superimposed on the image of the nucleus (A-D,G,H, panel c). In the case of RyR and IP_3R, the localization pattern of each protein was shown alone (E,F panels a and b, respectively), and when superimposed together and with the image of the nucleus (E,F panel d). Scale bars, 5 μm. (Ad-Dd,Ee,Fe,Gd,Hd) Line-scan analyses. The 0 and 18 in panel Ac indicate the start and end point of the line-scan, which makes up the x-axis of panel Ad.*

experiments suggest that TPC2 is necessary for triggering and/or partially generating both the SP1 and SP2 Ca^{2+} signals.

The *TPCN2*-MO data were supported via a complementary pharmacological approach with bafilomycin A1 and *trans*-ned-19. In both cases, the drugs were applied after the start of the SP1, to ensure that the robust SP1 Ca^{2+} signaling signature was initiated normally before the experimental treatments in order to eliminate false negative results. In the bafilomycin A1 experiments, the Ca^{2+} signals generated at the end of SP1 and during the entire SP2 were largely eliminated, suggesting that Ca^{2+} release from the acidic stores might be crucial for the latter portion of the SP1 signaling and for the initiation of SP2 Ca^{2+} signaling. Furthermore, as the Ca^{2+} ATPase from the SR membrane has been reported to be only moderately sensitive to bafilomycin A1 (Bowman *et al*., 1988), this suggests that following bafilomycin A1 treatment, the SR should, therefore, still contain sufficient Ca^{2+} to generate a SR-mediated signal. As no signal was detected following treatment, this indicates that the TPC2-generated Ca^{2+} signal maybe upstream of any Ca^{2+} signal generated by the SR, suggesting that the former might act as a trigger. The effects of treatment were only seen ~30 min after the application of bafilomycin A1. This delay most likely represents the time required for the diffusion of bafilomycin A1 along the trunk, and thus for it to reach an effective inhibitory concentration in the anterior myotome. Furthermore, the decrease in SP1 Ca^{2+} signaling was observed to be gradual (Fig. 2 B,E). This may be due to the mode of action of bafilomycin A1, whereby the acidic stores are depleted in a progressive manner via the action of the drug on vacuolar-type H^+-ATPases. The H^+ gradient across the wall of the acidic organelles is thus disrupted, which results in the subsequent Ca^{2+} refilling processes being inhibited (Docampo and Moreno, 1999). Embryos were also treated with *trans*-ned-19 (Naylor *et al*., 2009). This again led to an attenuation of the late SP1 and the entire SP2 Ca^{2+} signals (Fig. 2Ci). Furthermore, as the SR Ca^{2+} store is not affected by *trans*-Ned-19, there should still be sufficient Ca^{2+} to generate a signal. The fact that all the Ca^{2+} signals were inhibited in the *trans*-Ned-19-treated embryos (as they were following treatment with bafilomycin A1), once again suggests that the TPC2-generated Ca^{2+} signal might be an upstream trigger of the SR-generated Ca^{2+} signals. Treatment with *trans*-ned-19 led to an abrupt, rather than gradual, decrease in the SP1 Ca^{2+} signal frequency (Fig. 2C,2F), perhaps because *trans*-ned-19 blocks NAADP-mediated Ca^{2+} release directly by high affinity binding to NAADP binding sites (Naylor *et al*., 2009). This is in contrast to the indirect action of bafilomycin A1, where the acidic Ca^{2+} stores are gradually depleted (Morgan *et al*., 2011).

Using a custom-made zebrafish anti-TPC2 antibody, we successfully established a temporal expression profile of TPC2 in SMCs in intact embryos (Fig. 3 Ai-Hii). Between ~16 hpf to 24 hpf, (i.e. the period when the adaxial cells (SMC progenitors) migrate and differentiate; Devoto *et al*., 1996); there was a gradual increase in the level of TPC2 expression in SMCs. In addition, over time there was a transition in the pattern of expression of TPC2; such that between ~16 hpf to 18 hpf, it was expressed in a homogeneous punctate pattern (Fig. 3 Aii, Bii, Aiv, Biv), and then between ~20 hpf and 24 hpf a distinct banding pattern developed (Fig. 3 Cii-Eii, Civ-Eiv). The absence of TPC2 expression following MO-mediated TPC2-knockdown (Fig. 3H ii,iv) and the presence of TPC2 expression following *TPC2* mRNA rescue (Fig. 3I ii,iv) confirms the antigen-specificity of the TPC2 antibody used.

We also prepared cultures of primary zebrafish muscle cells to investigate the subcellular localization of TPC2 (Figs. 4, 5). In this system, we again showed that there was a transition from a homogeneous and punctate TPC2 labeling pattern in the forming myofibers after ~24 h in culture, to a far more organized pattern of localization characterized by distinct sarcomeric banding after ~48 h in culture (Fig. 4Bb,4Be). We estimate, therefore, that the stage of myogenesis following ~24 h and ~48 h of primary culture is approximately equivalent to the early (i.e. ~18 hpf to 20 hpf) and late (i.e. ~20 hpf to 24 hpf) stages of SMC myogenesis *in vivo*, respectively. Such an *in vitro* to *in vivo* developmental stage comparison is also supported by the localization patterns of IP_3R and RyR in SMCs (compare Fig. 4 D,E, with Fig. 13 of Cheung *et al*., 2011). Taken together, our immunolabeling studies suggest a changing pattern of TPC2 localization that might imply different signaling functions for TPC2 as the SMCs differentiate.

In muscle cell cultures, TPC2 labeling was localized adjacent to the sarcomeric I-band region, which contains the Z-disc (Fig. 4B). The Z-disc contains a significant number of proteins, and is thought to serve as a nodal point for signal transduction (Frank *et al*., 2006), as well as being important for structural and mechanical stability (Luther, 2009). Several Ca^{2+}-sensitive proteins are known to be associated with the Z-disc. These include calcineurin (Knöll *et al*., 2002) and muscle lim protein (Arber *et al*., 1994). Such proteins may therefore act as potential targets of TPC2-mediated Ca^{2+} signaling during early myogenesis, and thus contribute to excitation-transcription (ET)-coupling, one of the proposed functions of the early SP1 (Cheung *et al*., 2011). The tight correlation between the TPC2/LAMP1 banding and I-band location (Fig. 4 B,C), also suggests a role for TPC2-mediated Ca^{2+} release in excitation-contraction (EC)-coupling, one of the major functions proposed for the later SP2 Ca^{2+} signals.

Rotation of the dual-labeled confocal stacks of SMCs in intact embryos and in culture (Figs. 3L and 4 F,G), suggests that the TPC2 and LAMP1 labeling is superficial to the myosin labeling. When stacks from intact zebrafish were rotated (Fig. 3L), there was more TPC2 labeling on the lateral side (i.e., closest to the skin) than on the medial side (i.e., closest to the neural tube and notochord) of the myofibrils within the SMCs, which indicates a possible asymmetrical distribution of TPC2-bearing lysosomes in the intact myotome. In the case of SMCs cultured on coverslips, stack rotation also suggested an asymmetry in both the superficial TPC2 and LAMP1 distribution with respect to the central myosin labeling (Fig. 4F, 4G). This again might reflect the asymmetry displayed in the intact zebrafish. What is also clear is the positioning of the TPC2/LAMP1 labeling adjacent to the I-band, and the close juxtapositioning of the TPC2/LAMP1 labeling next to that of the myosin filaments. We suggest that these structures are separated by the SR, and that their close association supports the proposition that TPC2-mediated Ca^{2+} release might act as trigger for a combination of RyR/IP_3R-mediated Ca^{2+} release from the SR that contributes to EC-coupling (Kinnear *et al*., 2004). Indeed, the close association between TPC2 and RyR shown by our immunolabeling data at 48 h (Fig. 4Df, 4Dg), indicates that TPC2 might directly interact with RyR in some manner, as has been previously suggested (Kinnear *et al*., 2008). RyR-mediated Ca^{2+}-induced Ca^{2+} release (CICR) may then propagate across the SMC SR, and in some cases perhaps also engage/recruit IP_3R to help extend the spread of Ca^{2+} release. This latter suggestion is supported by our RyR and IP_3R type III

dual labeling results, where the lateral boundaries of the IP_3R type III striations extend beyond those of the RyR (Fig. 4Ef, 4Eg). The idea that NAADP-evoked Ca^{2+} release might act to trigger CICR via RyR and IP_3R was first proposed by Cancela *et al.,* (1999), when they demonstrated that mouse pancreatic acinar cells are more sensitive to NAADP than they are to either cADPR or IP_3, and that NAADP stimulated the production of a series of Ca^{2+} spikes of both short and longer duration.

Evidence is accumulating to suggest that NAADP regulates Ca^{2+} release via TPCs located on acidic organelles during differentiation of skeletal muscle precursors and C2C12 cells (Aley *et al*., 2010). It has previously been shown that acidic organelles are located near the t-tubules at the level of the I-band in the skeletal muscle fibers of frog *in vitro* (Krolenko *et al*., 2006). In both frog and fish, the t-tubules are located approximately adjacent to the Z-disc in skeletal muscle fibers (Davis and Carson, 1995; Zhang *et al*., 2009). This is consistent with our observation that TPC2/LAMP1 labeling is localized adjacent to the I-band, which contains the Z-disc. Furthermore, our labeling experiments show that in zebrafish SMCs, all three Ca^{2+} release channels, (i.e., TPC2, RyR and IP_3R Type III) are localized adjacent to the I-band (Fig. 4B, 4D and 4E).

Nuclear and peri-nuclear localization of TPC2 and LAMP1 was observed in ~24 h primary cultures, i.e., equivalent to SMCs *in vivo* at ~18 hpf (Fig. 5A a-c, C a-c). This indicates that lysosomes containing TPC2 are in close proximity to the nuclear region at the time of SMC differentiation. Furthermore, we have also shown that IP_3R type III and RyR are both localized in the peri-nuclear regions in SMC primary cultures at around the same time (Fig. 5E). We have previously reported that in intact zebrafish, SMCs generate both nuclear and cytoplasmic Ca^{2+} signals at ~18.5 hpf (Cheung *et al*., 2011). Our new observations suggest that TPC2-mediated Ca^{2+} signaling might also trigger RyR and/or IP_3R type III Ca^{2+} release in and around the nucleus during early myogenesis. It has been previously proposed that the low frequency, high amplitude component of the Ca^{2+} signaling signature seen during the early SP1 of zebrafish SMCs, are generated by IP_3R located around the nucleus (Cheung *et al*., 2011). This proposition is supported by a number of reports from mammalian systems where IP_3R are localized in the nuclear regions of SMCs (Jaimovich *et al*., 2000), and IP_3R-mediated Ca^{2+} signals are generated during ET-coupling in cultured skeletal muscle cells via the activation of transcriptional activators such as cyclic-AMP response element-binding protein (CREB; Cárdenas *et al*., 2005). Our findings thus implicate a possible role for TPC2 in nuclear Ca^{2+} signaling, perhaps acting as an upstream trigger for IP_3R-mediated Ca^{2+} signals during ET-coupling. The first evidence of NAADP-induced Ca^{2+} release from the nucleus was described in the isolated neurons of *Aplysia* (Bezin *et al*., 2008). More recently, TPCs have been reported to be associated with the peri-nuclear zone in mouse spermatids, where they play a role in Ca^{2+} release during the acrosome reaction (Arndt *et al*., 2014).

It has been previously shown that during the early larval stage of zebrafish development, only a few SMCs in each somite are specifically innervated by primary motor neurons (Eisen *et al*., 1986), yet all the SMCs in one somite, as well as those in adjacent somites, signal together (Cheung *et al*., 2011), supporting the suggestion that they are electrically coupled in some manner (Luna and Brehm, 2006). This coupling might serve to propagate waves of depolarization that activate a component in the sarcolemma that stimulates the production of NAADP. This, therefore, might explain the preferential location of LAMP1/TPC2 labeling adjacent to the sarcomeric I-bands and their associated t-tubules. These regions might represent SMC trigger zones where NAADP-mediated Ca^{2+} release from TPC2 initiates CICR via RyR and perhaps also via IP_3R type III located in the SR membrane, thus generating the crucial EC-coupled Ca^{2+} signal.

Conclusions

Our study suggests a key role for TPC2-mediated Ca^{2+} release during the generation of distinct patterns of Ca^{2+} signaling associated with ET- and EC-coupling in SMCs during myogenesis in intact zebrafish embryos. It has been suggested that both forms of coupling are essential for SMC differentiation (Brennan *et al*., 2005; Cheung *et al*., 2011). Our Ca^{2+} signaling and immunolabeling experiments suggest the establishment of trigger zones where TPC2 is initially co-localized with RyR and IP_3R type III in the nucleus and peri-nuclear domain to primarily trigger ET signals. They subsequently also become localized into distinct striated banding patterns along with RyR and IP_3R adjacent to sarcomeric I-bands in the cytoplasmic domain of SMCs, forming additional trigger zones to regulate EC-coupling, what we suggest is the major function of SP2. Involving TPCs in the signal transduction pathway may take advantage of the potency of NAADP, which is effective at pM or low nM concentrations (Galione and Ruas, 2005). The precise signal transduction pathways that stimulate the contraction of SMCs during SP1 and SP2 are not yet fully understood due to the complexity of both muscle fiber and primary neuron development along with the formation of neuromuscular junctions (Flanagan-Steet *et al*., 2005). We propose that the aforementioned potency of NAADP is a key element in ensuring that the essential ET-/EC-coupled signals are generated and perceived before the precise innervation of the myotome by primary and secondary motor neurons is completed (Eisen *et al*., 1986). This study thus suggests the operation of an essential developmental and functional Ca^{2+} signaling pathway that utilizes both acidic- and SR-located Ca^{2+} stores (as well as the interaction of three distinct intracellular Ca^{2+} mobilizing channels), with a primary role for NAADP-mediated Ca^{2+} release coordinating Ca^{2+} release from the SR, which operates during early SMC formation in intact zebrafish.

Materials and Methods

Zebrafish husbandry and embryo collection

Wild-type (AB strain) zebrafish (*Danio rerio*) and the α-actin-apoaequorin-IRES-EGFP (α-actin-aeq) transgenic line (developed by Cheung *et al*., 2011) were held in system water maintained at ~28°C. The wild-type fish were obtained from the Zebrafish International Resource Centre (University of Oregon, Eugene, OR, USA). Fertilized eggs were collected and transferred to Danieau's solution and then maintained at ~28°C during experiments.

In vivo reconstitution of aequorin and bioluminescence-based Ca^{2+} imaging

A 10 mM stock solution of *f*-coelenterazine (NanoLight® Technologies, Pinetop, AZ, USA) was prepared using a 1:3 ratio of 1,2-propanediol (Acros Organics, Thermo Fisher Scientific, Geel, Belgium) and (2-hydroxypropyl)-β-cyclodextrin (Sigma-Aldrich Corp., MO, USA). *f*-coelenterazine was first dissolved in 1,2-propanediol after which (2-hydroxypropyl)-β-cyclodextrin was added, and the mixture was then sonicated for ~30 min at 4°C. The clear yellowish solution produced was stored at -80°C.

To reconstitute active aequorin *in vivo*, α-actin-aeq transgenic embryos were incubated in the dark at ~28°C with 50 μM *f*-coelenterazine in Danieau's solution from the ~8-cell to 64-cell stage (i.e., 1.25 hpf to 2 hpf) until the ~16-somite stage (~17 hpf). Embryos were incubated while still in their chorions, then briefly washed with Danieau's solution to remove residual *f*-coelenterazine prior to the start of the experiment. After washing, embryos were dechorionated manually as described previously (Cheung *et al.*, 2011). Dechorionated embryos were placed in custom-designed imaging chambers as previously described (Webb and Miller, 2013) before being transferred to one of our PMT-based systems (Science Wares, Inc., East Falmouth, MA, USA; Webb *et al.*, 2010) for luminescence detection. Following data collection, 1% Triton X-100 (Sigma-Aldrich Corp.) in Danieau's solution was used to lyse the embryo and "burn-out" residual aequorin as described previously (Cheung *et al.*, 2011).

Preparation of primary cell cultures

Intact embryos were maintained in Danieau's solution until the ~16-somite stage. They were then sterilized by washing, first with ~0.07% bleach in water and then with ~75% ethanol, each for ~30 seconds. Sterilized embryos were then transferred to Danieau's solution and dissected by removing the chorion and then separating the trunk from the rest of the embryo using a pair of micro-dissection scissors (World Precision Instruments, FL, USA). All the equipment was cleaned with ~75% ethanol prior to use. Dissected trunks were transferred to Custom ATV (aqueous trypsin and Versene®) solution (Andersen, 2002), containing 0.5 mM EDTA and 2% penicillin-streptomycin and incubated for ~20 min to facilitate cell dissociation at room temperature. The custom ATV solution was then removed, and the trypsinized trunk tissue was suspended in muscle culture medium (50% L-15; Gibco, 48% 0.1X Ringer's solution [116 mM NaCl, 2.9 mM KCl, 1.8 mM $CaCl_2 \cdot 2H_2O$, 5 mM HEPES], 1% fetal bovine serum and 1% penicillin-streptomycin) and triturated to facilitate cell dissociation further. To remove any residual custom ATV solution, the cell suspension was centrifuged at 1000 rpm for 5 min and the supernatant was discarded. The pellet was then re-suspended in muscle culture medium, after which the dissociated cells were plated onto glass coverslips (Precision cover glasses No. 1.5H; Paul Marienfeld GmbH & Co. KG) contained in a Nunc Nunclon® Δ Surface 4-well plate (Thermo Fisher Scientific). Cells were cultured at ~28°C for ~24 h or ~48 h, after which they were fixed with phosphate buffered saline (PBS; 137 mM NaCl, 2.68 mM KCl, 16 mM Na_2HPO_4, 4 mM $NaH_2PO_4 \cdot 2H_2O$, pH 7.3) containing 4% paraformaldehyde (PFA) for 15 min at room temperature prior to immunolabeling.

Immunocytochemistry and whole-mount immunohistochemistry

Primary cell cultures that were fixed as described above, were washed thoroughly with PBS and then permeabilized with PBS containing 0.1% triton X-100 (PBST) for 10 min, after which they were incubated with blocking solution (PBST containing 10% goat serum and 1% bovine serum albumin; BSA) for 30 min. Cells were then incubated sequentially with the 2137A rabbit anti-TPC2 antibody (used at 1:10; custom-made by CovalAb UK Ltd., Cambridge, UK) and either the F59 mouse anti-myosin heavy chain antibody (used at 1:10; Developmental Studies Hybridoma Bank, Iowa, USA) or the 34C mouse anti-ryanodine receptor (RyR) antibody (used at 1:500; Sigma-Aldrich Corp.). The F59 anti-myosin heavy chain antibody can be used to specifically identify SMCs in cells derived from early stage embryos (Devoto *et al.*, 1996). In some experiments, cells were co-labeled with an anti-LAMP1 antibody (used at 1:100; Abcam, Cambridge, UK) and F59; with anti-IP_3R type III antibody (used at 1:250; Sigma-Aldrich Corp) and the 34C anti-RyR antibody; or with F59 and either the anti-IP_3R type I antibody (used at 1:10; Calbiochem, Merck KGaA, Darmstadt, Germany) or the anti-IP_3R type II antibody (used at 1:10; Sigma-Aldrich Corp). TPC2, LAMP1 and IP_3R types I-III were then visualized with the Atto 647N goat anti-rabbit IgG (used at 1:200; Active Motif, Inc., Carlsbad, CA, USA) while the myosin heavy chain and RyR were visualized with an Alexa Fluor 488 goat anti-mouse IgG (H+L) antibody (used at 1:200; Molecular Probes Inc.). All antibody incubations were carried out for 1 h at room temperature and the secondary antibody incubations were performed in the dark. Between each antibody incubation step the cells were rinsed extensively with wash buffer (PBS-T containing 1% goat serum and 0.1% BSA) and following the final antibody incubation, cells were washed with PBST and then with Milli-Q water, after which they were mounted under ProLong Gold antifade reagent containing DAPI (Life Technologies).

For whole-mount immunolabeling, embryos at 24 hpf were dechorionated manually and then fixed with 4% PFA in PBS either overnight at 4°C or for 4 h to 6 h at room temperature. Fixation was conducted following anesthetization with 0.02% MS-222 in Danieau's solution. Embryos were labeled using well-established techniques (Cheung *et al.*, 2011), using the anti-TPC2 antibody and the F59 mouse anti-myosin heavy chain antibody, followed by the Atto 647N goat anti-rabbit IgG and Alexa Fluor 488 goat anti-mouse IgG (H+L) antibodies, described previously. At the end of immunolabeling, the yolk and head of labeled embryos were excised and the trunk was mounted under AF1 mountant (Citifluor Ltd., Leicester, UK).

Imaging immunolabelled embryos and primary cultured cells

Fluorescently-labeled embryos and cells were imaged using a Leica TCS SP5 II confocal system. Images were acquired using both the multi-photon mode as well as the normal confocal mode, using HCX PL APO 63X/1.4-0.6 NA and HCX PL APO 100X/1.4 NA oil immersion objective lenses. Alexa Fluor 488 fluorescence was captured using 488 nm excitation and 519 nm detection; Atto 647 fluorescence was captured with 633 nm excitation and 669 nm detection; and DAPI fluorescence was captured via 780 nm multi-photon excitation and 461 nm detection using a BP 460/50 filter cube and a Hamamatsu/Leica non-descanned detector.

To study the localization of antibody labeling, the fluorescence intensity profile of different channels of selected images was plotted using ImageJ. This software was also used to rotate stacks of optical sections by 90° horizontally and/or vertically in order to investigate the localization of TPC2 and LAMP1 (in cultured muscle cells) and TPC2 (in intact embryos) with regards to the myosin heavy chain in more detail. Numerical data were exported from ImageJ to Microsoft Office Professional Plus Excel 2010 for graph plotting and statistical analysis, and CorelDRAW X5 was used for figure preparation.

Pharmacological treatments

Stock solutions of the vacuolar-type H^+ ATPase inhibitor, bafilomycin A1 (Calbiochem, Merck KGaA, Darmstadt, Germany), and the NAADP receptor inhibitor, *trans*-ned-19 (Enzo Life Sciences, Inc., Farmingdale, NY, USA; Naylor *et al.*, 2009), were prepared at 500 μM or at 40 mM in DMSO, respectively, and stored at -20 °C. To facilitate drug diffusion into the muscle tissues of the later-stage (i.e., 16 hpf to 19 hpf) embryos, the terminal tail buds of the embryos were excised using a 27G ½ tungsten needle just prior to drug treatment (Liu and Westerfield, 1990; Cheung *et al.*, 2011). Transgenic embryos were incubated in 1 μM of bafilomycin A1, ~250 μM *trans*-ned-19 or 1.25% DMSO (control) in Danieau's solution in the dark at ~28°C between ~18 hpf to ~18.5 hpf (i.e., shortly after the SMC Ca^{2+} signals have been reported to begin; Cheung *et al.*, 2011) until the end of Ca^{2+} imaging (i.e., at ~30 hpf).

Design and injection of morpholino oligomers

All morpholino oligomers (MOs; prepared by Gene Tools LLC, Philomath, OR, USA) were prepared at a stock concentration of 1 mM in Milli-Q water and kept at room temperature. The expression of TPC2 was attenuated using a *TPCN2*-MO. As some MOs are known to induce p53 activity and thus result in non-specific apoptosis (Robu *et al.*, 2007; Manning *et al.*, 2010; Klüver *et al.*, 2011) the *TPCN2*-MO was co-injected with a previously characterized *p53*-MO (Robu *et al.*, 2007) at a ratio of ~1:1.5. The *p53*-MO (injected alone) and a standard control-MO were also used as specificity controls. ~1.5 nL of the diluted MOs were injected into the yolk of embryos at the 1-cell to 4-cell stage. Embryos were microinjected using equipment and methods described previously (Webb and Miller, 2013). The sequences for the *TPCN2*-, *p53*- and standard control-MOs used, are as follows:

TPCN2-MO(ATG): 5'-CAGCCAGCAGCGGTTCTTCTTCCAT-3'
p53(ATG)-MO: 5'-GCGCCATTGCTTTGCAAGAATTG-3'
Standard control-MO: 5'-CCTCTTACCTCAGTTACAATTTATA-3'

Cloning and design of mRNA rescue construct

The *TPCN2* IMAGE clone (3816064) was purchased from Geneservice (Geneservice Ltd, Cambridge, UK) and was subcloned into the PCRIITOPO vector. The following primers were used:
Forward primer:
CAACGCTCTGTTTGGGATTT
Reverse primer:
GCCTACACAGACGTGATGGA
This vector served as a backbone for generating an mRNA rescue construct in which two silent mutations in the *TPCN2* coding sequence were introduced using the QuickChange II Site-Directed Mutagenesis kit (Stratagene, La Jolla, CA, USA). The primers used for silent mutant cloning were as follows:
Forward primer:
TAGATGGAGGAGGAACCGCTGCTGGCTGGCAGCATTAAC
Reverse primer:
CGGTTCCTCCTCCATCTAAACGGCTGCAAGTGTCCTACA
The third base of the second and third codons was mutated. The sequence for the rescue construct is as follows (mutations are underlined):
TPCN2-mRNA: 5'-ATGGAGGAGGAACCGCTGCTGGCTG-3'
In order to generate the silent mutant mRNA sequence that still encodes a wild type protein but is unrecognizable by the *TPCN2*-MO, the modified *TPCN2* cDNA clone was first incorporated into competent *E. coli* (cmk strain) via transformation. Subsequently, plasmids were isolated using a Mini Plus TM Plasmid DNA Extraction System (Viogene BioTek Corp., Taipei, Taiwan) and then linearized using a Kpn1 restriction enzyme (New England Biolabs Inc., MA, USA) prior to *in vitro* transcription using a mMESSAGE mMACHINE T7 transcription kit (Ambion, Invitrogen Corp.). The rescue construct generated was then diluted to ~250 ng/μL in Milli Q containing diethylpyrocarbonate (DEPC) and kept at -80 °C. During rescue experiments, a mixture of the *TPCN2*- and *p53*-MOs was first injected into the yolk of embryos at the 1-cell stage, after which ~50 pg to ~100 pg *TPCN2*-mRNA was immediately injected into the blastodisc, to reverse the knock-down effect of the *TPCN2*-MO. For Ca^{2+} measurements, α-actin-aeq transgenic embryos were then bathed in *f*-coelenterazine as described previously (Webb and Miller, 2013).

Acknowledgements

ALM was funded by The Hong Kong Research Grants Council General Research Fund awards HKUST662211, 662113, and 16101714; the ANR/RGC Joint Research Scheme award A-HKUST601/13; and the Hong Kong Theme-based Research Scheme award T13-706/11-1. AG and JP were in receipt of a program grant (ref: 084102/Z/07/Z) from the Wellcome Trust. We thank David Whitmore and Peter Cormie (UCL, UK) for their muscle cell culture protocol. Thanks also to Michael Granato (UPenn, PA, USA) and Robert Baker (NYU, USA) for their advice regarding neuronal innervation.

References

ALEY, P.K., MIKOLAJCZYK, A.M., MUNZ, B., CHURCHILL, G.C., GALIONE, A. and BERGER, F. (2010). Nicotinic acid adenine dinucleotide phosphate regulates skeletal muscle differentiation via action of two-pore channels. *Proc Natl Acad Sci USA* 107: 19927–19932.

ANDERSEN, S.L. (2002). Preparation of dissociated zebrafish spinal neuron cultures. *Meth Cell Sci* 23: 205–209.

ARBER, S., HALDER, G. and CARONI, P. (1994). Muscle LIM protein, a novel essential regulator of myogenesis, promotes myogenic differentiation. *Cell* 79: 221–231.

ARNDT, L., CASTONGUAY, J., ARLT, E., MEYER, D., HASSAN, S., BORTH, H., ZIERLER, S., WENNEMUTH, G., BREIT, A., BIEL, M., *et al.,* (2014). NAADP and the two-pore channel protein 1 participate in the acrosome reaction in mammalian spermatozoa. *Mol Biol Cell* 25: 948–964.

BERRIDGE, M.J. (2012). Calcium signaling, remodeling and disease. *Biochem Soc Trans* 40: 297-309.

BOOTMAN, M.D., BERRIDGE, M.J. and RODERICK, H.L. (2002). Calcium signalling: more messengers, more channels, more complexity. *Curr Biol* 12:R563–R565.

BEZIN, S., CHARPENTIER, G., LEE, H.C., BAUX, G., FOSSIER, P. and CANCELA, J.M. (2008). Regulation of nuclear Ca^{2+} signaling by translocation of the Ca^{2+} messenger synthesizing enzyme ADP-ribosyl cyclase during neuronal depolarization. *J Biol Chem* 283: 27859-27870.

BRENNAN, C., MANGOLI, M., DYER, C.E. and ASHWORTH, R. (2005). Acetylcholine and calcium signaling regulates muscle fibre formation in the zebrafish embryo. *J Cell Sci* 118: 5181–5190.

BOWMAN, E.J., SIEBERS, A. and ALTENDORF, K. (1988). Bafilomycins: A class of inhibitors of membrane ATPases from microorganisms, animal cells, and plant cells. *Proc Natl Acad Sci USA* 85: 7972-7976.

CALCRAFT, P.J., RUAS, M., PAN, Z., CHENG, X., ARREDOUANI, A., HAO, X., TANG, J., RIETDORF, K., TEBOUL, L., CHUANG, K.T., *et al.,* (2009). NAADP mobilizes calcium from acidic organelles through two-pore channels. *Nature* 459: 596–600.

CANCELA, J.M., CHURCHILL, G.C., and GALIONE, A. (1999). Coordination of agonist-induced Ca^{2+}-signalling patterns by NAADP in pancreatic acinar cells. *Nature* 398: 74-76.

CANG, C., ZHOU, Y., NAVARRO, B., SEO, Y.J., ARANDA, K., SHI, L., BATTAGLIA-HSU, S., NISSIM, I., CLAPHAM, D.E. and REN, D. (2013). mTOR regulates lysosomal ATP-sensitive two-pore Na^{+} channels to adapt to metabolic state. *Cell* 152: 778–790.

CÁRDENAS, C., LIBERONA, J.L., MOLGO, J., COLASANTE, C., MIGNERY, G.A. and JAIMOVICH, E. (2005). Nuclear inositol 1,4,5-trisphosphate receptors regulate local Ca^{2+} transients and modulate cAMP response element binding protein phosphorylation. *J Cell Sci* 118: 3131-3140.

CHEUNG, C.Y., WEBB, S.E., LOVE, D.L. and MILLER, A.L. (2011). Visualization, characterization and modulation of Ca^{2+} signaling during the development of slow muscle cells in intact zebrafish embryos. *Int J Dev Biol* 55: 153–174.

CHURCHILL, G.C., OKADA, Y., THOMAS, J.M., GENAZZANI, A.A., PATEL, S. and GALIONE, A. (2002). NAADP mobilizes Ca^{2+} from reserve granules, lysosome-related organelles, in sea urchin eggs. *Cell* 111: 703–708.

DAVIS, A.K. and CARSON, S.S. (1995). Proteoglycans are present in the transverse tubule system of skeletal muscle. *Matrix Biol.* 14: 607–621.

DEVOTO, S.H., MELANÇON, E., EISEN, J.S. and WESTERFIELD, M. (1996). Identification of separate slow and fast muscle precursor cells *in vivo*, prior to somite formation. *Development* 122: 3371–3380.

DOCAMPO, R. and MORENO, S.N. (1999). Acidocalcisome: A novel Ca^{2+} storage compartment in trypanosomatids and apicomplexan parasites. *Parasitol Today* 15: 443–448.

DU, S.J., DEVOTO, S.H., WESTERFIELD, M. and MOON, R.T. 1997. Positive and negative regulation of muscle cell identity by members of the hedgehog and TGF–β gene families. *J Cell Biol* 139: 145–156.

EISEN, J.S., MYERS, P.Z. and WESTERFIELD, M. (1986). Pathway selection by growth cones of identified motoneurones in live zebra fish embryos. *Nature* 320: 269–271.

FLANAGAN-STEET, H., FOX, M.A., MEYER, D. and SANES, J.R. (2005). Neuromuscular synapses can form *in vivo* by incorporation of initially aneural postsynaptic specializations. *Development* 132: 4471-4481.

FRANK, D., KUHN, C., KATUS, H.A. and FREY, N. (2006). The sarcomeric Z-disc: a nodal point in signalling and disease. *J Mol Med* 84: 446–468.

GALIONE, A. and RUAS, M. (2005). NAADP receptors. *Cell Calcium* 38: 273–280.

JAIMOVICH, E., REYES, R., LIBERONA, J.L. and POWELL, J.A. (2000). IP_3 receptors, IP_3 transients, and nucleus-associated Ca^{2+} signals in cultured skeletal muscle. *Am J Physiol Cell Physiol* 278:C9980–C1010.

JHA, A., AHUJA, M., PATEL, S., BRAILOIU, E. and MUALLEM, S. (2014). Convergent regulation of the lysosomal two-pore channel-2 by Mg^{2+}, NAADP, $PI(3,5)P_2$ and multiple protein kinases. *EMBO J* 33: 501–511.

KINNEAR, N.P., BOITTIN, F.X., THOMAS, J.M., GALIONE, A. and EVANS, A.M. (2004). Lysosome-sarcoplasmic reticulum junctions. *J Biol Chem* 279: 54319–54326.

KINNEAR, N.P., WYATT, C.N., CLARK, J.H., CALCRAFT, P.J., FLEISCHER, S., JEYAKUMAR L.H., NIXON, G.F. and EVANS, A.M. (2008). Lysosomes co-localize with ryanodine receptor subtype 3 to form a trigger zone for calcium signaling by NAADP in rat pulmonary arterial smooth muscle. *Cell Calcium* 44: 190–201.

KLÜVER, N., YANG, L., BUSCH, W., SCHEFFLER, K., RENNER, P., STRÄHLE, U.

and SCHOLZ, S. (2011). Transcriptional response of zebrafish embryos exposed to neurotoxic compounds reveals a muscle activity dependent *hspb11* expression. *PLoS ONE* 6:e29063.

KNÖLL, R., HOSHIJIMA, M. and CHIEN, K.R. (2002). Z-line proteins: implications for additional functions. *Eur Heart J Suppl* 4:I13–I17.

KROLENKO, S.A., ADAMYAN, S.Y., BELYAEVA, T.N. and MOZHENKO, T.P. (2006). Acridine orange accumulation in acid organelles of normal and vacuolated frog skeletal muscle fibers. *Cell Biol Int* 30: 933–939.

LIU, D.W. and WESTERFIELD, M. (1990). The formation of terminal fields in the absence of competitive interactions among primary motoneurons in the zebrafish. *J Neurosci* 10: 3947–3959.

LUNA, V.M. and BREHM, P. (2006). An electrically coupled network of skeletal muscle in zebrafish distributes synaptic current. *J Gen Physiol* 128: 89–102.

LUTHER, P.K. (2009). The vertebrate muscle Z-disc: sarcomere anchor for structure and signaling. *J Muscle Res Cell Motil* 30: 171–185.

MANNING, J.A., LEWIS, M., KOBLAR, S.A. and KUMAR, S. (2010). An essential function for the centrosomal protein NEDD1 in zebrafish development. *Cell Death Diff* 17: 1302-1314.

MENTEYNE, A., BURDAKOV, A., CHARPENTIER, G., PETERSEN, O.H. and CANCELA, J.M. (2006) Generation of specific Ca^{2+} signals from Ca^{2+} stores and endocytosis by differential coupling to messengers. *Curr Biol* 16: 1931-1937.

MORGAN, A.J. and GALIONE, A. (2014). Two-pore channels (TPCs): Current controversies. *Bioessays* 35: 1–11.

MORGAN, A.J., PLATT, F.M., LLOYD-EVANS, E. and GALIONE, A. (2011). Molecular mechanisms of endolysosomal Ca^{2+} signalling in health and disease. *Biochem. J* 439: 349-374.

NAYLOR, E., ARREDOUANI, A., VASUDEVAN, S.R., LEWIS, A.M., PARKESH, R., MIZOTE, A., ROSEN, D., THOMAS. J.M., IZUMI, M., GANESAN, A., *et al.,* (2009). Identification of a chemical probe for NAADP by virtual screening. *Nat Chem Biol* 5: 220–226.

PARRINGTON, J. and TUNN, R. (2014). Ca^{2+} signals, NAADP and two-pore channels: role in cellular differentiation. *Acta Physiol* 211: 285-296.

RINGER, S. (1882). Concerning the influence exerted by each of the constituents of the blood on the contraction of the ventricle. *J Physiol (Lond)* 3: 380–383.

ROBU ME, LARSON JD, NASEVICIUS A, BEIRAGHI, S., BRENNER, C., FARBER, S.A. and EKKER, S.C. (2007). p53 activation by knockdown technologies. *PLoS Genet* 3:e78.

RUAS, M., CHUANG, K-T., DAVIS, L.C., AL-DOURI, A., TYNAN, P.W., TUNN, R., TEBOUL, L., GALIONE, A. and PARRINGTON, J. (2014). TPC1 has two variant isoforms and their removal has different effects on endo-lysosomal functions compared to loss of TPC2. *Mol Cell Biol* 34: 3981-3992.

TUGBA DURLU-KANDILCI, N., RUAS, M., CHUANG, K.T., BRADING, A., PARRINGTON, J. and GALIONE, A. (2010). TPC2 proteins mediate nicotinic acid adenine dinucleotide phosphate (NAADP)- and agonist-evoked contractions of smooth muscle. *J Biol Chem* 285: 24925–24932.

WANG, X., ZHANG, X., DONG, X. P., SAMIE, M., LI, X., CHENG, X., GOSCHKA, A., SHEN, D., ZHOU, Y. and HARLOW, J., *et al.,* (2012). TPC proteins are phosphoinositide-activated sodium-selective ion channels in endosomes and lysosomes. *Cell* 151: 372–383.

WEBB, S.E. and MILLER, A.L. (2013). Microinjecting holo-aequorin into dechorionated and intact zebrafish embryos. *Cold Spring Harb Protoc* 5: 447–455.

WEBB, S.E., ROGERS, K.L, KARPLUS, E. and MILLER, A.L. (2010). The use of aequorins to record and visualize Ca^{2+} dynamics: from subcellular microdomains to whole organisms. *Meth Cell Biol* 99: 263–300.

ZHANG, R., YANG, J., ZHU, J. and XU, X. (2009). Depletion of zebrafish Tcap leads to muscular dystrophy via disrupting sarcomere-membrane interaction, not sarcomere assembly. *Hum Mol Genet* 18: 4130–4140.

Further Related Reading, published previously in the *Int. J. Dev. Biol.*

Egg activation in physiologically polyspermic newt eggs: involvement of IP3 receptor, PLCγ, and microtubules in calcium wave induction
Tomoyo Ueno, Takehiro Ohgami, Yuichirou Harada, Shuichi Ueno and Yasuhiro Iwao
Int. J. Dev. Biol. (2014) 58: 315-323

Visualization, characterization and modulation of calcium signaling during the development of slow muscle cells in intact zebrafish embryos
Chris Y. Cheung, Sarah E. Webb, Donald R. Love and Andrew L. Miller
Int. J. Dev. Biol. (2011) 55: 153-174

Could modifications of signalling pathways activated after ICSI induce a potential risk of epigenetic defects?
Brigitte Ciapa and Christophe Arnoult
Int. J. Dev. Biol. (2011) 55: 143-152

Oscillatory Ca2+ dynamics and cell cycle resumption at fertilization in mammals: a modelling approach
Geneviève Dupont, Elke Heytens and Luc Leybaert
Int. J. Dev. Biol. (2010) 54: 655-665

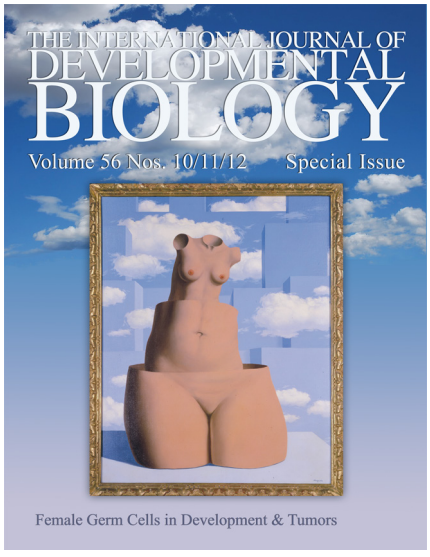

The role of ion fluxes in polarized cell growth and morphogenesis: the pollen tube as an experimental paradigm
Erwan Michard, Filipa Alves and José A. Feijó
Int. J. Dev. Biol. (2009) 53: 1609-1622

Sperm-activating peptides in the regulation of ion fluxes, signal transduction and motility
Alberto Darszon, Adán Guerrero, Blanca E. Galindo, Takuya Nishigaki and Christopher D. Wood
Int. J. Dev. Biol. (2008) 52: 595-606

The dynamics of calcium oscillations that activate mammalian eggs
Karl Swann and Yuansong Yu
Int. J. Dev. Biol. (2008) 52: 585-594

The choice between epidermal and neural fate: a matter of calcium.
Marc Moreau and Catherine Leclerc
Int. J. Dev. Biol. (2004) 48: 75-84